Neurobiology of Disease 139 (2020) 104787

Contents lists available at ScienceDirect

Neurobiology of Disease

journal homepage: www.elsevier.com/locate/ynbdi

Transient upregulation of translational efficiency in prodromal and early symptomatic Tg2576 mice contributes to Aβ pathology

Antonella Borreca[a,b,*], Francesco Valeri[c], Mariassunta De Luca[c], Lysianne Ernst[d], Arianna Russo[e], Annalisa Nobili[c,f], Alberto Cordella[c,f], Veronica Corsetti[g], Giuseppina Amadoro[g,h], Nicola Biagio Mercuri[c,i], Marcello D'Amelio[c,f], Martine Ammassari-Teule[c,j,**]

[a] Institute of Neuroscience-National Research Council (CNR), Via Vanvitelli, 32 20129 Milano, Italy
[b] Humanitas University, Department of Biomedical Sciences, Via Rita Levi Montalcini 4, 20090 Pieve Emanuele – Milan, Italy
[c] IRCCS Fondazione Santa Lucia, Centro Europeo di Ricerca sul Cervello (CERC), via del Fosso di Fiorano, 64, 00143 Rome, Italy
[d] University of Namur, Faculty of Sciences, Belgium
[e] INGM National Institute of Molecular Genetic, Via Francesco Sforza, 35–20122 Milano, Italy
[f] Unit of Molecular Neurosciences, Department of Medicine, University Campus-Biomedico, via Alvaro del Portillo, 21 00128 Rome, Italy
[g] EBRI FOUNDATION, Viale Regina Elena, 295 Roma, Italy
[h] IFT-CNR, Via Fosso del Cavaliere, 100 - 00133 Roma, Italy
[i] University of Rome "Tor Vergata", 00133 Rome, Italy
[j] Institute of Biochemistry and Cellular Biology (IBBC), CNR Via Ercole Ramarini 32, 00015 Monterotondo Scalo (Roma), Italy.

ARTICLE INFO

Keywords:
Alzheimer's disease
Tg2576 mice
hAPP mRNA
eIF2α
Translational control
Salubrinal
Pre-symptomatic markers
Cognition
Synaptic plasticity

ABSTRACT

TG2576 mice show highest levels of the full length mutant Swedish Human Amyloid Precursor Protein (APPKM670/671LN) during prodromal and early sympotomatic stages. Interestingly, this occurs in association with the unbalanced expression of two of its RNA Binding proteins (RBPs) opposite regulators, the Fragile-X Mental Retardation Protein (FMRP) and the heteronuclear Ribonucleoprotein C (hnRNP C). Whether an augmentation in overall translational efficiency also contributes to the elevation of APP levels at those early developmental stages is currently unknown. We investigated this possibility by performing a longitudinal polyribosome profiling analysis of APP mRNA and protein in total hippocampal extracts from Tg2576 mice. Results showed that protein polysomal signals were exclusively detected in pre-symptomatic (1 months) and early symptomatic (3 months) mutant mice. Differently, hAPP mRNA polysomal signals were detected at any age, but a peak of expression was found when mice were 3-month old. Consistent with an early but transient rise of translational efficiency, the phosphorylated form of the initial translation factor eIF2α (p-eIF2α) was reduced at pre-symptomatic and early symptomatic stages, whereas it was increased at the fully symptomatic stage. Pharmacological downregulation of overall translation in early symptomatic mutants was then found to reduce hippocampal levels of full length APP, Aβspecies, BACE1 and Caspase-3, to rescue predominant LTD at hippocampal synapses, to revert dendritic spine loss and memory alterations, and to reinstate memory-induced c-fosactivation. Altogether, our findings demonstrate that overall translation is upregulated in prodromal and early symptomatic Tg2576 mice, and that restoring proper translational control at the onset of AD-like symptoms blocks the emergence of the AD–like phenotype.

Abbreviations: hAPP, human amyloid precursor protein; APP, amyloid precursor protein; FMRP, fragile X mental retardation protein; hnRNPC, heterogeneous nuclear ribonucleoprotein C (C1/C2); eIF2α, eukaryotic initiation factor 2 alpha; peIF2α, phosphorylated form of the eukaryotic initiation factor 2 alpha; eIF4G, eukaryotic translation initiation factor 4G; eIF4E, eukaryotic translation initiation factor 4E; BACE1, β-secretase 1; CASP-3, caspase-3; DMSO, dimethyl sulfoxide; GDP, guanosin diphosphate; GTP, Guanosine Triphosphate; DHPG, 3,5-diidrossifenilglicina

* Correspondence to: Institute of Neuroscience (IN)-National Research Council (CNR), Via Vanvitelli, 32 20129 Milano, Italy.
** Corresponding author.
E-mail addresses: antonella.borreca@gmail.com, antonella.borreca@in.cnr.it, antonella.borreca@humanitasresearch.it (A. Borreca), martine.teule@cnr.it, annemarie.teule@cnr.it (M. Ammassari-Teule).

https://doi.org/10.1016/j.nbd.2020.104787
Received 19 August 2019; Received in revised form 14 January 2020; Accepted 31 January 2020
Available online 04 February 2020

1. Introduction

Overexpression of the amyloid precursor protein (APP) is a common feature of several intellectually disabling pathologies including Alzheimer's Disease (Tcw and Goate, 2017), Down syndrome (Head et al., 2018) and autism spectrum disorders (Sokol et al., 2006; Ray et al., 2011; Westmark, 2019; Westmark et al., 2016). In Alzheimer's Disease (AD), despite the observation of a direct link between increased levels of full length APP and elevated β-amyloid peptide (Aβ) production (Johnston et al., 1994), APP-related research has prevalently focused on the toxic role of its cleavage products. Evidence that functional changes occur in the brain long before the onset of cognitive deficits (Beason-Held et al., 2013; Pignataro et al., 2019) has, however, highlighted the need to identify increasingly earlier AD brain markers. Within this context, the dysregulation of APP levels upstream to its pathogenic proteolytic cleavage is gaining an increased interest (Zhu et al., 2019). Nevertheless, although epigenetic (Maloney and Lahiri, 2016) and post-transcriptional (Long et al., 2012) factors have been suggested to play a role in early-life APP regulation, the translational mechanisms which regulate APP expression at prodromal and early symptomatic stages of the disease remain largely unexplored.

In mouse models of familiar AD, overexpression of mutant forms of the human amyloid precursor protein (hAPP) promotes formation of toxic Aβ and impairs cognition at age points which vary according to the locus of the mutation in the APP gene and the number of hAPP transgene copies (Howlett and Richardson, 2009). For example, Tg2576 mice carrying the Swedish KM670/671LN mutation are cognitively intact at 2 months of age (D'Amelio et al., 2011). Then, cognition gradually declines around 3 months of age concurrently with the augmentation of Aβ load (D'Amelio et al., 2011; Lanté et al., 2015). Paradoxically, although the insertion of the hAPP transgene in the mouse genome warrants that APP is overexpressed from birth in this model, we reported that APP mRNA and protein hippocampal levels show significant fluctuations during the course of development (Borreca et al., 2016). Specifically, these levels are maximal when mice are asymptomatic (1 month of age), remain elevated at the onset of mild cognitive impairments (3 months of age), and then decrease with the emergence of the full symptomatology (6 months of age). We also noticed that the prodromal/early symptomatic upregulation of APP levels occurs when the heteronuclear Ribonucleoprotein C (hnRNP C) and the Fragile-X Mental Retardation Protein (FMRP), two post-translational opposite regulators of APP expression (Lee et al., 2010), are maximally up- and down-regulated respectively, and therefore favor APP mRNA-specific translation. Whether a prodromal/early symptomatic increase in overall translation also contributes to the elevation of full length APP levels is unknown.

To examine this point, we performed a longitudinal polysome profile analysis of APP mRNA and protein in Tg2576 mice and controlled for translational efficiency by measuring eukaryotic initial translation factors at corresponding age points. Results showed that protein polysomal signals were exclusively detected in pre-symptomatic (2 months) and early symptomatic (3 months) mutant mice. Differently, mRNA polysomal signals were detected at any age, but a peak of expression was found when mice were 3-month old. Consistent with an early but transient rise of translational efficiency, the phosphorylated form of the initial translation factor eIF2α (p-eIF2α) was increased at pre-symptomatic and early symptomatic stages, whereas it was decreased at the fully symptomatic stage. Confirming that upregulation of overall translation contributes to emergence of AD pathogenic factors in Tg25756 mice, pharmacological restoration of proper translational control in early symptomatic mice blocked the emergence of their AD–like neural and cognitive phenotype.

2. Methods

2.1. Animals

Male mice overexpressing the APP695 fragment with the Swedish mutation subsequently backcrossed to C57BL/6 × SJL F1 females. The offspring was genotyped to confirm the presence of human mutant APP DNA sequence by PCR. Genomic DNA isolated from mouse tails was genotyped by polymerase chain reaction (PCR) analysis. Specific primers sense (5′-CTG ACC ACT CGA CCA GGT TCT GGG T-3′) and antisense (5′-GTG GAT AAC CCC TCC CCC AGC CTA GAC CA-3′) of APPSWE (10 μM each) were added into genomic DNA template mixtures that were subjected to 25 cycles of amplification. Amplification was conducted in a T100 thermal cycler (BioRad Laboratories Inc., Hercules, California, USA) under the following conditions: denaturation for 30 s at 94 °C, annealing for 30 s at 62 °C, and extension for 45 s at 72 °C. The amplified PCR products were then loaded onto a 1.0% agarose gel, after which the bands were detected using the Kodak Electrophoresis Documentation and Analysis System 120 (Eastman Kodak, Rochester, NY, USA). Mice were reared maintained on a 12 h light/dark cycle with ad libitum access to food and water. All experiments were performed in accordance with the guidelines provided by the European Communities Council Directive of 24 November 1986 (86/609/EEC).

2.2. Polyribosome profile

Polyribosome profiling allows to study the overall degree of translation of individual proteins and their mRNAs. Hippocampi from Tg2576 mice of 1, 3, and 6 months of age (pool of 4 animals for each age point) were homogenized in 0,5 ml of lysis buffer (100 mM NaCl, 10 mM $MgCl_2$, 10 mM Tris-HCl pH 7.5, 1% Triton-X100). The lysates were incubated 5 min in ice, centrifuged for 5 min at 12,000*g* at 4 °C, and the total amount of supernatants (cytoplasmic extract) centrifuged through 15%–50% (*w/v*) sucrose gradients for 180 min at 37,000 rpm in a Beckman SW41 rotor. The polysomes, the 80S monosome, the two subunits 60S and 40S as well as the very light mRNPs were detected by UV absorbance at 256 nm (BioRad) and each gradient was collected in 10 fractions. From each fraction, the proteins were precipitated with mix containing 50% Ethanol, 25% Methanol and 25% Acetone. The proteins extracted were resuspended in 30 μl of laemly buffer 2× and then analyzed by Western blotting.

2.3. Western blot determination of APP on polysome fractions

From each polysomal fraction, we used 200 μl for protein extraction. 200 μl of each fraction was treated with 6 volumes (1,2 ml) of mix containing 50% EtOH, 25% MetOH and 25% Acetone and left overnight a 4 °C. On the day after, each faction was centrifuged at 14000 *g* for 40 min and washed with 1 ml of EtOH 80%. The resulting pellet was resuspend in 30 μl of laemly buffer 2×. 10 μl of each fraction of polysomes gradient from WT and Tg2576 mice were used in this analysis. Total proteins were separated by 4–15% gradient sodium dodecyl sulfate–polyacrylamide gels (BIO-RAD Laboratories, Hercules, CA) and transferred to nitrocellulose membrane (BIO-RAD Laboratories, Hercules, CA). Western blots were blocked in 5% non-fat dry milk in TBST buffer (0.1% Tween 20 in Tris–borate saline) then incubated with APP (1:1000; Sigma). Blots were then incubated with appropriate conjugated to horseradish peroxidase (Chemicon) and developed by ECL Western Blotting Analysis System (GE Healthcare).

2.4. Real time-quantitative PCR for APP mRNA on polysome fractions

Cytoplasmic extracts prepared from hippocampi of Tg2576 mice were fractionated through sucrose gradients. Ten fractions were collected from each gradient while recording the absorbance profile. For

RNA purification, the fractions were immediately treated with a solution containing 1% SDS (final concentration), 10 μg of glycogen, 50 pg of kanamycin positive control RNA and 100 μg/ml of proteinase K, and then incubated for 30 min at 37 °C. Kanamycin synthetic RNAs were used to normalize for possible RNA loss during RNA phenol/chloroform extraction and precipitation from each fraction. RNAs were precipitated with 0.2 M NaOAc pH 4.8 and 0.7 volumes of isopropanol. The pellets, washed with EtOH 80%, were re-suspended in 20 μl of ddH2O. Total RNA extracted from each fractions was analyzed by quantitative RT-PCR for specific mRNAs (mouse and human APP). To correct for variations in the efficiency of the RT-PCR reaction, the same amount of a synthetic RNA (Kanamicin) was added to each sample, amplified, and used for normalization. 1 μl of each fraction were pulled to differentiate polysomes fractions (Fraction 1–5) and non polysomes fractions (Fraction 6–10). 5 μl of each fraction (polysomes and non polysomes) was used for First-strand synthesis using p(dN)6 and 100 U of M-MLV RT (Invitrogen). The same amount of first strand DNA was used for qRT-PCR analysis. The qRT-PCR was conducted with SYBR green master mix (Applied Biosystem) and specific primer for APP mRNA and Kanamycin synthetic DNA.

2.5. Western blot determination of eukaryotic initial translation factors

Hippocampi from WT and Tg2576 mice were collected at each age point of interest and homogenized in RIPA buffer (10 mM Tris-HCl, pH 7.5, 150 mM NaCl, 2% Nonidet P-40, 5 mM EDTA, 0.1 mM phenylmethylsulfonyl fluoride, 1 mM β-glycerophosphate, 1 mM sodium orthovanadate, 10 mM sodium fluoride, 0.1 M SDS, 1% protease inhibitor cocktail-Sigma Aldrich) (Borreca et al., 2018). A pool of 4 animals was used for the analysis. To confirm these data a four WT and Tg2576 mice were loaded on acrylamide gel separately. 50 μg of proteins were loaded on 12% acrylammide gel and transferred on nitrocellulose membrane, blocked with 5% not fat milk and incubated with p-eIF2α and eIF2α antibodies (Cell signaling) over night at 4 °C (diluted in BSA 5%). After three washes with TBST, the membranes were incubated with secondary antibody HRP, specific for both primary antibodies and the signal was revealed by ECL Western Blotting Analysis System (GE Healthcare). Additional p-eIF4E, eIF4E and eIF4G antibodies (Cell signaling) were used to determine the level of these two other major eukaryotic initial translation factors in the hippocampus of 3-month old Tg2576 mice.

2.6. Pharmacological treatment

Pharmacological inhibition of elF2α (eukaryotic translation initiation factor 2 subunit alpha) dephosphorylation was carried out by injecting salubrinal (Tocris Cat. No. 2347) emulsified in DMSO (Sigma) (1% diluted in saline). Two administration routes were used according to previously established injection protocols (Sokka et al., 2007). Mice were given either one intra-cerebro-ventricular (i.c.v.) injection (1 μl of a 75 μM solution) or one daily intraperitoneal (i.p.) injection repeated for 7 consecutive days (1 mg/kg). Control mice received i.c.v. or i.p. injections of DMSO.

2.7. Western blot determination of APP, Aβ and BACE-1 levels in hippocampal extracts

Hippocampi of WT and Tg2576 mice, treated with salubrinal or DMSO, were lysed with RIPA buffer (10 mM Tris-HCl, pH 7.5, 150 mM NaCl, 2% Nonidet P-40, 5 mM EDTA, 0.1 mM phenylmethylsulfonyl fluoride, 1 mM β-glycerophosphate, 1 mM sodium orthovanadate, 10 mM sodium fluoride, 0.1 M SDS, 1% protease inhibitor cocktail-(Sigma Aldrich, see Borreca et al., 2016). After homogenization, samples were centrifuged at 12,000*g* for 10 min and the supernatant was collected, quantified with Bradford assay, and 50 μg of total protein were loaded on 12% acrylamide gel for determination of APP (Sigma), Amyloid-β (Aβ peptide species (D54D2 Cell Signaling), β-secretase enzyme-1 (BACE-1, Millipore).

2.8. Western blot for determination of Caspase-3 activity in hippocampal synaptosomes

Hippocampi of WT and Tg2576 mice treated with salubrinal or DMSO were lysed with Homogenization buffer (320 mM sucrose, 4 mM Hepes pH 7.4, 1 mM EGTA, 1 mM PMSF and 1× protease inhibitor cocktail). The homogenized tissue was centrifuged at 1000 *g* for 10 min a 4 °C. the supernatant was collected and centrifuged at 12,000*g* for 15 min at 4 °C. The obtained pellet was resuspended in homogenization buffer and centrifuge at 13,000*g* for 15 min at 4 °C. The pellet was resuspended in RIPA buffer (10 mM Tris-HCl, pH 7.5, 150 mM NaCl, 2% Nonidet P-40, 5 mM EDTA, 0.1 mM phenylmethylsulfonyl fluoride, 1 mM β-glycerophosphate, 1 mM sodium orthovanadate, 10 mM sodium fluoride, 0.1 M SDS, 1× protease inhibitor cocktail-Sigma Aldrich). The resuspended pellets was sonicated and centrifuged at 12,000 rpm for 10 min at 4 °C. The synaptosomes were loaded on acrylammide gel and the CASP3 (Cell signaling) levels (cleaved/total, D'Amelio et al., 2011) was evaluated. The primers and second antibodies used in this experiment are listed in Table 1.

2.9. Specification of primers and antibodies

Primers and antibodies used in these experiments are listed in Table 1.

2.10. Acute slices preparation for electrophysiology

Mice were deeply anesthetized by inhalation of 2-Bromo-2-Chloro-1,1,1-trifluoroethane and after decapitation the brains were rapidly removed from the skull. Parasagittal slices were cut with a vibratome (VT1200S, Leica) and then immersed in chilled bubbled (95% O2, 5% CO2) aCSF containing (in mM): NaCl 124, KCl 3, NaH_2PO_4 1.25, $NaHCO_3$ 26, $MgCl_2$ 1, $CaCl_2$ 2, glucose 10 (~290 mOsm, pH 7.4). The slices were incubated for 1 h in CSF at 32 °C and then left at room

Table 1
List of antibodies and primers used for the experiments.

Antibodies	Company	Code	Species	Secondary antibodies
APP	Sigma	A8717	Human and mouse	Antirabbit
p-eIF2α	Cell Signaling	#9721	H M R Mk Dm	Anti-Rabbit
eIF2α	Cell Signaling	#9722	H M R Mk	Anti Rabbit
eIF4E	Cell Signaling	#9742	H M R Mk Mi Z	Anti Rabbit
eIF4G	Cell Signaling	#2498	H M R Mk	Anti Rabbit
Aβ	Cell Signaling	#D54D2	H	Anti Rabbit
BACE1	Millipore	MAB5308 clone61-3E7	H, M, R, Pm	Anti Mouse
CASP3	Cell Signaling	#9662	H M R Mk	Anti Rabbit

Gene	Primers	Species
FOR genotyping	5′-CTG ACC ACT CGA CCA GGT TCT GGG T-3′	
FOR genotyping	5′-GTG GAT AAC CCC TCC CCC AGC CTA GAC CA-3′	
hAPP FOR	5′-GCCAAAGAGACATGCAGTGA-3′	Human
hAPP REV	5′-AGTCATCCTCCTCCGCATC-3′	Human
mAPP FOR	5′-GACAAGAAGGCCGTTATCC-3′	Mouse
mAPP REV	5′-GTCTCTCATTGGCTGCTTTCC-3′	Mouse
GAPDH FOR	5′-GTGAACGGATTTGGCCGTAT-3′	Mouse
GAPDH REV	5′-GAATTTGCCGTGAGTGGAGT-3′	Mouse
KANAMYCIN FOR	5′-GCC ATT CTC ACC GGA TTC AGT CGTC-3′	Synthetic RNA
KANAMYCIN REV	5′-AGCCGCCGTCCCGTCAAGTCAG-3′	Synthetic RNA

Table 2
Variations in p-eIF2α levels reported in TG mice and AD patients. If detected in tissues from patients with mild cognitive impairment (MCI), the opposite dysregulation of APP and p-eIF2α levels might identify MCI-AD converters (Vignini et al., 2013).

	Early symptomatic	Symptomatic
AD mice	APP ⇧ p-eIF2α ⇩ [present study]	APP ⇧ p-eIF2α ⇧ [Kim et al., 2007; present study]
	MCI converters	**AD diagnosis**
AD patients	APP ⇧ [Vignini et al., 2013] p-eIF2α ?	APP ⇧ p-eIF2α ⇧ [Chang et al., 2002;Ma et al., 2013]

temperature for 30 min before recordings (Table 2).

2.11. Field recordings of excitatory postsynaptic potentials

A single brain slice was transferred to a recording chamber of an upright microscope (Axioskop 2-FS; Zeiss, Germany) and completely submerged in aCSF (3–4 ml/min; 32 °C). Field excitatory postsynaptic potential (fEPSP) were induced by stimulation (100 μs duration; every 30 s) of Schaffer collateral pathway using a concentric bipolar stimulating electrode (FHC Inc.; Bowdoin, ME) and a CSF-filled borosilicate glass recording electrode that were positioned in the stratum radiatum of the CA1 hippocampal region at a distance of 200–300 μm. All experiments were performed at the intensity yielding a half-maximal response of input-output curves that was obtained by measuring the fEPSP initial slope at increasing 10 μA steps of afferent stimulation (D'Amelio et al., 2011).

2.12. Long term depression

LTD was induced 20 min after the test stimulation (at half-maximal intensity, every 30 s) when fEPSP slope stability was obtained. The slice was challenged with DHPG (50 μM) for 10 min and then washed out for 60 min. The DHPG-LTD was evaluated by the fEPSP mean slope 55–60 min from DHPG washout, normalized to the mean slope during baseline, and recorded during the 10 min preceding DHPG perfusion. The field responses were recorded with a MultiClamp 700B amplifier and digitized with Digidata 1322A. Data were sampled at 20 kHz. Traces were obtained by pClamp 9.2 and analyzed using Clampfit 9.2 (all from Molecular Devices; Sunnyvale, CA).

2.13. Golgi staining

After one week of pharmacological treatment with salubrinal or DMSO, mice were deeply anesthetized with a cocktail of Zoletil (800 mg/kg) and Rompum (200 mg/kg) and perfused transcardially with 0.9% saline solution ($N = 7$ mice per group). Brains were dissected and immediately immersed in a Golgi-Cox solution (1% potassium dichromate, 1% mercuric chloride, and 0.8% potassium chromate) at room temperature for 6 days according to a previously described protocol (Gibb and Kolb, 1998). On the seventh day, brains were transferred in a 30% sucrose solution for cryoprotection and then sectioned with a vibratome. Coronal sections (100 μm) were collected and stained according to the method described by Gibb and Kolb (1998). Sections were stained through consecutive steps in water (1 min), ammonium hydroxide (30 min), water (1 min), developer solution (Kodak fix 100%, 30 min), and water (1 min). Sections were then dehydrated through successive steps in alcohol at rising concentrations (50%, 75%, 95%, and 100%) before being closed with slide cover slips. Spine density was analyzed on CA1 neurons. Neurons were identified with a light microscope (Leica DMLB) under low magnification (20×/NA 0.5). Five neurons within each hemisphere were taken from each animal. On each neuron, five 30–100 μm dendritic segments of secondary and tertiary branch order of CA1 dendrites were randomly selected and counted using Neurolucida software. Only protrusions with a clear connection of the head of the spine to the shaft of the dendrite were counted as spines. Statistical comparisons were made on single neuron values obtained by averaging the number of spines counted on segments of the same neuron. The analysis was conducted by an experimenter blind to the experimental condition.

2.14. Novel object recognition

The novel object recognition (NOR) test was carried out in 3-month old Tg2576 and WT mice. Testing started on the day after mice received the last i.p. injections of salubrinal or DMSO. Mice in their home cage were transferred to experimental room and left to acclimate for 1 h to the new environment. NOR testing consisted in three sessions (Fig. 5A). On the first session (open field exploration), each mouse was placed in an empty squared open field (40 cm in side) surrounded by 60 cm-high walls and left free to explore it for 10 min. The mouse was returned to its home cage for a 10-min pause during which two identical glass cylinders of 3 cm in diameter and 10 cm in height (object on the left: sx; object on the right: dx) were put in opposite corners of the open field. On the second session (training), the mouse was placed in the center of the open field and allowed to explore objects sx and dx for 10 min. The mouse was returned again to its home cage for a 1 h-pause during which one (sx or dx) familiar object (FO) was substituted with a novel object (NO), a multicolored kubrik cube of 5 cm in side (NO). On the third session (testing), the mouse was placed again the center of the open field and allowed to explore the FO and the NO for 10 min. Object exploration was defined as mice sniffing or touching the object with its nose and/or forepaws. The objects were cleaned with 10% ethanol between each session. The preference index was calculated according the formula previously described (Antunes and Biala, 2012) which estimates the percentage of time spent exploring each object (FO or NO) over the total time spent exploring both objects. A preference index above 50% indicates a preference for the NO, below 50% a preference for the FO, and 50% no preference.

2.15. NOR-induced c-fos activation

1 h following NOR testing, mice were deeply anesthetized with mix solution of ketamina/xylazin (100 mg/kg) and immediately perfused with PAF 4% according to a procedure previously described (Borreca et al., 2018). The brains were immediately removed, post-fixed in PAF 4% overnight, transferred in sucrose (30% diluted in PBS1×), and then sectioned coronally with a cryostat (40 μm). Slices were immediately washed with PBS 1× and incubated with primary antibody (*c-fos* 1:400) diluted in a solution of PBS 1× and 0.3% Triton overnight at 4 °C. After incubation, the slices were immediately washed with PBS 1× and incubated with specific secondary antibody (Alexa Fuor 555 antirabbit) for 2 h at room temperature avoiding light. DAPI staining (1:1000, Enzo Life Science) was performed at the last wash with PBS 1×. Sections were mounted with fluoromount (Sigma) and

coverslipped. The staining was visualized at confocal microscope (Zeiss LSM700; magnification 20×) and images were analyzed with IMARIS software. The number of *c-fos* immunoreactive spots in the CA1 hippocampus were counted in 10 areas of 25 × 25 μm were analyzed avoiding the DAPI. Number of spots for WT and Tg2576 mice were counted compared between groups.

2.16. Statistical analyses

Group differences in hippocampal APP mRNA polysome gradient distribution and in p-eiF2α/eiF2α ratio were evaluated by means of two-way ANOVAs with genotype and age point as main factors. Student's *t*-tests (two-tailed) for unpaired samples were used to evaluate the effect of genotype on p-eIF4E/eIF4E and eIF4G levels, and the effect of the injection route (i.p. vs i.c.v.) on APP and Aβ levels in the hippocampus of 3-month old Tg2576 mice. In mice of the same age receiving i.p. DMSO or salubrinal injections, differences in hippocampal levels of p-eIF2α, APP, BACE-1, in the cCASP-3/Casp-3 ratio measured in hippocampal synaptosomes, and in dendritic spines, LTD, and NOR-induced *c-fos* activation measured in the CA1 region of the hippocampus were statistically evaluated by means of two way ANOVAs with genotype and treatment as main factors. Student's t-tests for paired samples were used to estimate object novelty preference in each experimental condition. Post-hoc pair comparisons were carried out where necessary by means of the Bonferroni and Fischer test. Statistical levels of significance were set at $P < .05$.

3. Results

3.1. APP mRNA and protein polysomal signals were exclusively detected in pre-symptomatic and early- symptomatic Tg2576 mice

As shown in Fig. 1A, an APP signal was detected in both polysome (lanes 1–5) and non-polysome (lanes 6–10) fractions in 1-month old Tg2576 mice. A weaker polysomal signal was still present in 3-month old Tg2576 mice, but no longer present when they were 6-month old. No polysomal signal was detected in WT mice at any age. The L7 distribution was also evaluated (data not shown). Of note, non-polysomal signals (lane 8–10) were decreased in both genotypes at 6 months of age.

A reliable way to assess mRNA translational efficiency is to analyze its partitioning between actively translating polysomes and mRNPs that are not translated. Total RNA was extracted from the gradient fractions and then analyzed by quantitative RT-PCR for hAPP mRNAs. Data are shown in Fig. 1B and are expressed as density levels of mRNA in polysomal vs non polysomal fraction (pool of four mice from each genotype reproduced three times). A two-way ANOVA performed on these data revealed a significant genotype x age interaction ($F_{(2,12)} = 326{,}42$; $p < 0{,}001$). Post hoc pair comparisons showed that hAPP mRNA was significantly more localized in the polysomal fraction when Tg2576 mice were 1-month ($p < .01$) and 3-month ($p < 0.01$) old, but equally distributed in polysomal and non polysomal fractions when mice were 6-month old ($p = .75$), the latter observation being in line with data obtained in 9-month old mice bearing the triple APP/Tau/PS1 mutation (Caccamo et al., 2015).Thus, the major presence of hAPP mRNA in polysomal fractions strictly associates with the upregulation of protein expression which occurs before or shortly after mice exhibit signs of cognitive deterioration. Of note, mouse APP (mAPP) was more localized on non polysomal fractions in both genotypes (Supplementary Fig. 1).

3.2. Tg2576 mice show early upregulation and late downregulation of translation

The eukaryotic initiation factor-2α (eIF2α) is an essential factor for protein synthesis. Extensive evidence suggests that its aberrant phosphorylation induces synaptic failure and neurodegeneration through persistent inhibition of mRNA translation. In line with this hypothesis, Kim et al. (2007) showed that p-eIF2α is upregulated in hippocampi homogenates from fully symptomatic 12-month-old Tg2576 mice. Interestingly, we confirm the p-eIF2α upregulation in hippocampal extracts from 6- and 9-month old symptomatic mice, but provide evidence of its downregulation at earlier stages of development (Fig. 2A-B). A two-way ANOVA performed on p-eIF2α levels measured in both genotypes at four age points revealed a significant genotype × age point interaction ($F_{(3,16)} = 77{,}40$, $p < .001$). Post hoc pair comparisons then showed significant differences between genotypes at all age points which developed, however, in opposite directions according to the age point. Specifically, p-eIF2α levels were lower in Tg2576 than in WT mice at 1 month ($p < .03$) and 3 months ($p < .01$) of age, but, consistent with previous data (Kim et al., 2007), these levels were higher in Tg2576 than in WT mice at 6 months ($p < .04$) and 9 months ($p < .02$) of age. These findings were confirmed by immunofluorescence detection of eIF2α phosphorylation expression in hippocampal sections taken from Tg2576 and WT mice at the same age points (Fig. 2C). Of note, the non-phosphorylated form of eIF2α did not vary between genotypes when mice were examined at 1 month ($p = .79$) and 3 months ($p = .18$) of age, but was decreased in mutant mice compared to WT mice at 6 months ($p < .04$) and the 9 months ($p = .05$) age concurrently with the increase in the phosphorylated form. Altogether, these results reveal the existence of non-linear variations of peIF2α hippocampal levels in Tg2576 mice which are consistent with an early upregulation followed by a downregulation of the protein synthesis machinery. Total blot of p-eIF2α (A-B) are shown in Supplementary Fig. 2.

3.3. p-eIF4E/eIF4E and eIF4G are unaltered in early symptomatic Tg2576 mice

Eukaryotic translation initiation factor 4E (eIF4E) is a rate-limiting component of the eukaryotic translation apparatus. This factor is specifically involved in the mRNA-ribosome binding step of eukaryotic protein synthesis of cap-dependent translation so that the majority of cellular mRNA requires eIF4E to be translated into proteins (Richter and Sonenberg, 2005). In the 48S initiation complex, a role for the eIF4G subunit of eIF4F has also been documented (Grüner et al., 2016). Specifically, eIF4G is a scaffold protein that binds eIF4E and serves as a central ribosome adaptor module which attracts 40S ribosomal subunits to the 5′ end of mRNAs via direct association with eIF3. We therefore measured the hippocampal levels of the phosphorylated and non-phosphorylated forms of eIF4E, and the levels of eIF4G in hippocampal extracts from 3-month old Tg2576 mice. Results (Fig. 2D-E) showed that none of these pre-initiation component of translation was altered in this genotype x age condition (p-eIF4E/eIF4E: $t_{(9)} = 0{,}47$, $p = 0{,}65$; eIF4G: $t_{(4)} = 0{,}94$, $p = 0{,}40$). Total blots for eIF4E (D), eIF4G (E) are shown in Supplementary Fig. 2.

3.4. Salubrinal reduces hippocampal APP and Aβ species levels

Salubrinal is a selective inhibitor of cellular complexes that dephosphorylate eIF2α and therefore decreases overall translation. Having shown that APP and Aβ levels are increased at ages where p-eIF2α phosphorylation is reduced, we have examined the possibility that i.c.v. or i.p. injections of the inhibitor of eIF2α dephosphorylation, salubrinal, could decrease abnormally elevated APP and Aβ levels. Western blot were carried out in hippocampal extracts from 3-month old Tg2576 mice treated with the compound or the vehicle (DMSO). Data are shown in Fig. 3. Statistical comparison of densitometric quantification of APP (Fig. 3A) and Aβ species (Fig. 3B) revealed that these levels were significantly lower in salubrinal-injected mice compared with DMSO-injected mice irrespective of the injection route [APP, i.c.v. $t_{(10)} = 2{,}71$, $p < .02$; i.p. $t_{(8)} = 2{,}54$, $p \leq .03$; Aβ, icv:

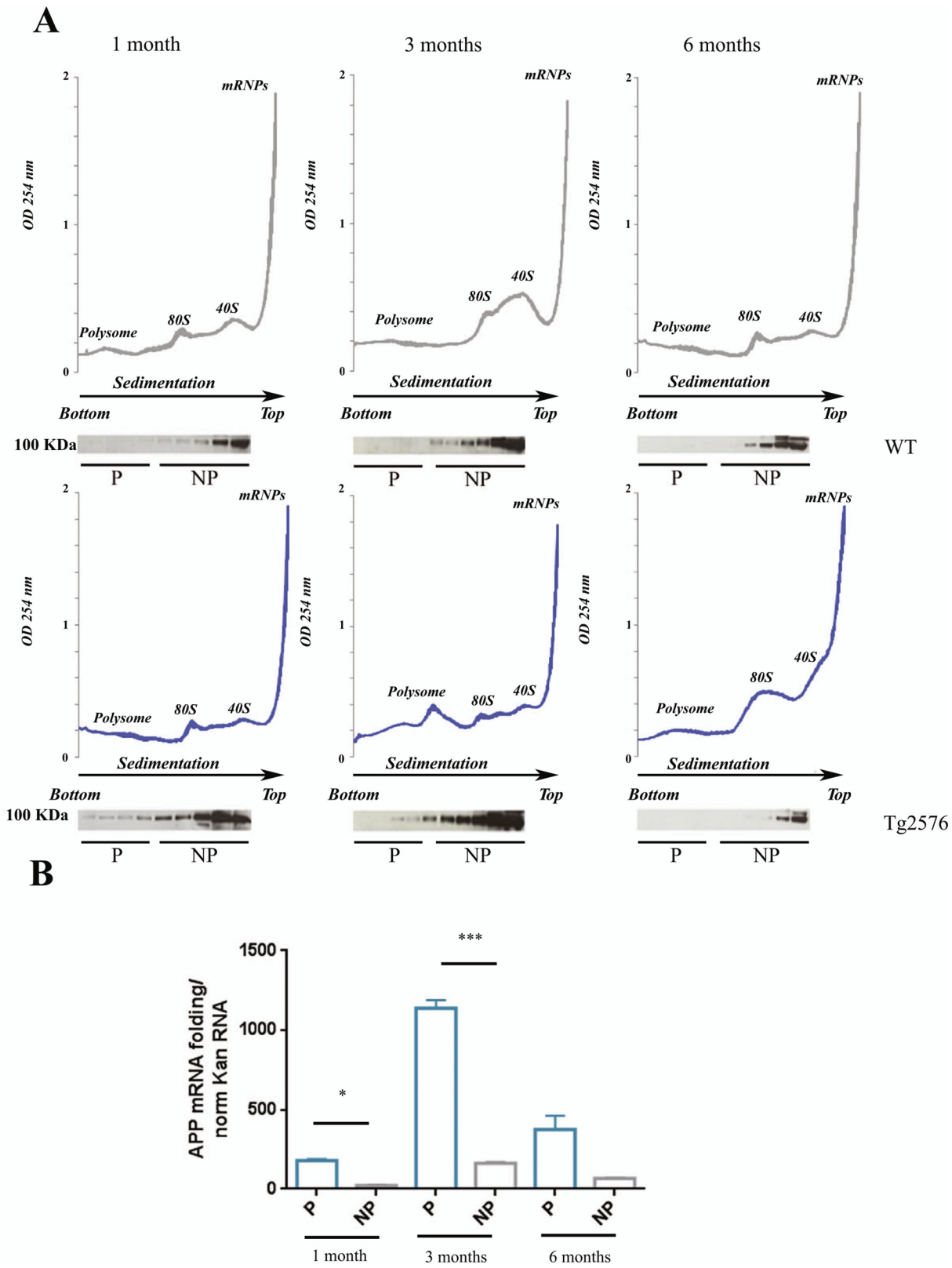

Fig. 1. Polysomal gradient fractionation of APP mRNA and protein from hippocampal extracts isolated from wild-type and Tg2576 mice of 1, 3, and 6 months of age. (**A**) Polysomal profile obtained from cytoplasmic brain extracts from wild-type mice (upper panels, grey lines) and Tg2576 mice (lower panels, blue lines). Brain extracts were centrifuged through a 15–50% sucrose gradient; absorbance at 254 nm was monitored continuously and plotted against the fraction numbers. The bottom fraction (heavy) includes fractions 1–5 and corresponds to polysomes (P). The top fraction (light) includes fractions 6–10 and corresponds to non polysomes (NP) with 80S, 60S 40S and mRNPs particles. (B) Histograms showing the distribution of hAPP mRNA on P and NP fractions after further processing of total RNA from each fraction by RT–qPCR (normalization with the synthetic RNA Kanamicin). Bars represent mean ± SEM.*$p < .05$ for WT vs Tg2576. (For interpretation of the references to colour in this figure legend, the reader is referred to the web version of this article.)

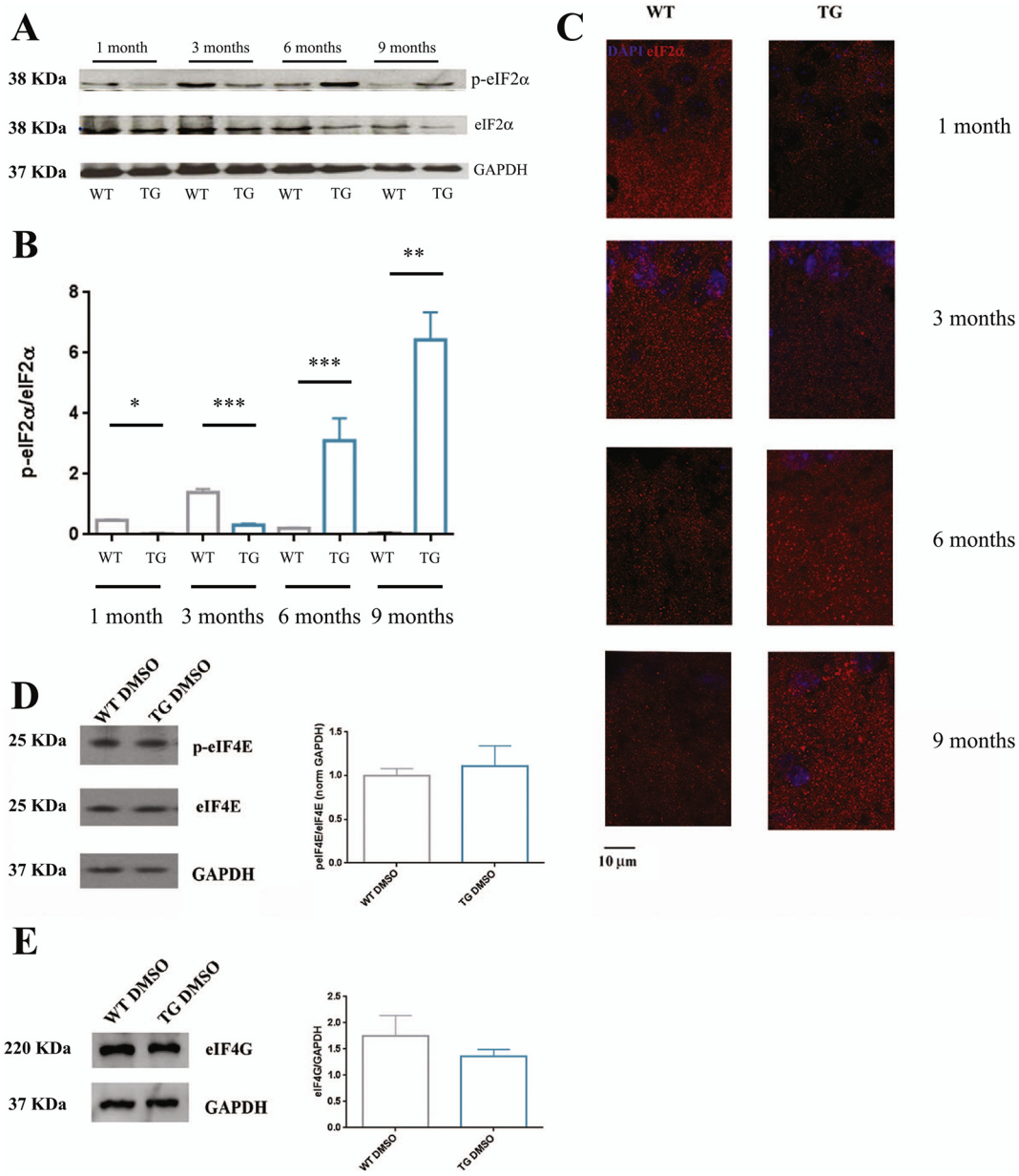

Fig. 2. Hippocampal eIF2α levels in wild-type and Tg2576 mice across development. (**A**) Western blot analysis of phosphorylated and non-phosphorylated eIF2α levels normalized for GADPH in the hippocampus of wild-type mice and Tg2576 mice of 1, 3, 6, and 9 months of age. (**B**) Histograms showing variations of the peiF2α/eiF2α ratio in the hippocampus of the same mice groups. (**C**) Immunofluorescence visualization of hippocampal p-eiF2α levels in the same mice groups. The two analyses show that hippocampal p-eiF2α levels were decreased in pre-symptomatic (1 month) and early symptomatic (3 months) Tg2576 mice, but were increased in symptomatic (6 and 9 months) Tg2576 mice relative to age-matched wild-type mice. *$p < .05$; **$p < .01$, ***$p < .001$. Histograms showing **(D)** peIF4E/eIF4E and **(E)** eIF4G levels measured in the hippocampus of 3-month old wild-type and Tg2676 mice. No difference in the expression level of these two eukaryotic translation initiation factors was detected between genotypes. Bars represent mean ± SEM. wild-type mice: grey bars; Tg2576 mice: blue bars. (For interpretation of the references to colour in this figure legend, the reader is referred to the web version of this article.)

$t_{(11)} = 2{,}20$; $p = .049$; i.p.: $t_{(4)} = 3{,}33$, $p < .03$). Of note for potential translational applications, i.p. injections were as much efficient as i.c.v. injections in decreasing hippocampal APP and Aβ levels. This observation prompted us to use the less invasive injection route for subsequent evaluation of the salubrinal rescuing effects on molecular, neural and cognitive alterations in early symptomatic mice. Total blot of of APP (A) and Aβ (B) are shown in Supplementary Fig. 3.

3.5. Salubrinal restores proper levels of p-eIF2α, APP, BACE1 in hippocampal extracts from early symptomatic Tg2576 mice

The verification that salubrinal rescues early upregulation of translation requires to show that the compound increases p-eIF2α levels of Tg2576 mice up to the levels of WT mice. Results are shown in Fig. 3C. Statistical comparisons showed a main effect of genotype ($F_{(1,10)} = 9{,}93$; $p < .01$), of treatment ($F_{(1,10)} = 15{,}77$; $p < .001$) and of the genotype x treatment interaction ($F_{(1,10)} = 5{,}21$; $p < .05$). Post hoc comparisons first confirmed our previous observation in non-treated mice (see Fig. 2) that p-eIF2α levels in the DMSO condition are significantly lower in Tg2576 mice than in WT mice ($p < .05$). As shown in Fig. 3C, salubrinal increased p-eIF2α in both genotypes (salubrinal vs DMSO WT mice, $p < .001$; salubrinal vs DMSO Tg2576 mice, $p < .05$). Remarkably, eIF2α levels were similar in salubrinal Tg2576 and DMSO WT mice ($p > 1$). For APP (Fig. 3D), we found a

significant genotype × treatment interaction ($F_{(1,5)} = 27.73$; $p < .01$). In the DMSO condition, APP levels were higher in Tg2576 mice than in WT mice ($p < .05$). Salubrinal decreased APP in the mutant mice (DMSO vs salubrinal Tg2576 mice, $p < 0.01$) to the level of DMSO-injected mice (salubrinal Tg2576 mice vs DMSO WT mice, $p = .27$). BACE1 is the first cleaving enzyme in the APP amyloid pathway. Extensive evidence show that BACE-1 inhibitors decrease Aβ load and reduce neuro-inflammation in fully symptomatic transgenic AD mice (Neumann et al., 2015). Differently, mixed effects were reported in AD patients especially when these inhibitors were administered peripherally (Georgievska et al., 2015). Here we show that salubrinal treatment decreased and increased BACE-1 levels in Tg2576 mice and WT mice respectively (Fig. 3E). A two-way ANOVA revealed a significant effect of genotype ($F_{(1,7)} = 6,15$; $p < .05$) and genotype x treatment interaction ($F_{(1,7)} = 79,93$, $p < .01$). Post hoc comparisons showed that BACE-1 levels were higher in DMSO Tg2576 than in DMSO WT mice ($p < .03$), but that the treatment was efficient in decreasing BACE-1 levels of Tg2576 mice to those of DMSO WT mice ($p = .42$). Total blots for p-eIF2α (C), APP (D) and BACE-1 (E) are shown in Supplementary Fig. 3.

3.6. Salubrinal rescues AD-selective caspase-3 alteration in hippocampal synaptosomes from early symptomatic Tg2576 mice

Caspase-3 (Casp-3) activity is significantly increased at hippocampal synapses of Tg2576 mice where it causes permanent activation of calcineurin which leads to dephosphorylation of the AMPA receptor GluR1 subunit and its removal from postsynaptic sites (D'Amelio et al., 2011). Because protein synthesis is required for Casp-3 activation (Coxon et al., 1998), we examined the possibility that salubrinal-mediated decrease of eIF2α phosphorylation, which reduces protein translation, could normalize Casp-3 levels in the mutant mice. Results are shown in Fig. 3F. In line with this hypothesis, statistical comparison of the cCasp-3/Casp-3 ratio measured in the four mice groups revealed a significant genotype x treatment interaction ($F_{(1,8)} = 1,13$ $p = .01$). Pair comparisons then showed that these levels were reduced in salubrinal Tg2576 mice compared to DMSO Tg2576 mice ($p = .01$) and were not different from those detected in DMSO WT mice ($p = .99$). To our knowledge, these data provide the first in vivo demonstration that, as in vitro (Gong et al., 2015), salubrinal is efficient in decreasing apoptosis markers at hippocampal synapses. Total blots for Caspase-3 (F) are shown in Supplementary Fig. 3.

3.7. Effect of salubrinal in WT mice

Consistent with a previous report (Mouton-Liger et al., 2012) that increasing eIF2α phosphorylation in healthy mice augments BACE-1 levels and induces Aβ amyloidogenesis, higher levels of BACE-1 ($p < .01$) (Fig. 3E) and p-eIF2α ($p < .01$) (Fig. 3C) were detected in WT mice treated with salubrinal compared to the WT mice treated with DMSO.

3.8. Salubrinal reverts synaptic plasticity alterations

At 3 months of age, Tg2576 mice show an increased magnitude of DHPG-induced long-term depression (LTD) at CA3-CA1 hippocampal synapses (D'Amelio et al., 2011). We applied the same LTD induction protocol in acute hippocampal slices obtained from Tg2576 and WT mice treated with salubrinal or DMSO. The data are shown in Fig. 4A–C. A two-way ANOVA carried out on relative changes of fEPSP slopes before and after low frequency stimulation in DMSO- and salubrinal-injected Tg2576 (Fig. 4A) and WT (Fig. 4B) mice revealed a significant genotype × treatment interaction ($F_{(1,35)} = 16.87$; $p < .01$). Pair comparisons of LTD percentage data (Fig. 4C) showed that DMSO-injected Tg2576 mice exhibited a significant increase in the magnitude of CA3-to-CA1 LTD compared to DMSO-injected WT mice ($p < .001$) which was rescued by salubrinal treatment (salubrinal Tg2576 vs DMSO Tg2576 mice, $p < .001$; salubrinal Tg2576 mice vs DMSO WT mice, $p > 1$). Dendritic spines are among the first synaptic elements which are disrupted during AD-related cognitive decline (Scheff et al., 2007). In Tg2576 mice, spine density in CA1 pyramidal neurons is significantly decreased at 3 months of age (D'Amelio M et al., 2011). We measured spine density in Golgi-stained pyramidal CA1 neurons from Tg2576 and WT mice treated with salubrinal and DMSO. Statistical comparison of spine density revealed a significant genotype x treatment interaction ($F_{(1,10)} = 27.37$; $p = .01$). Pair comparisons of spine scores showed that DMSO-injected Tg2576 mice exhibited a significant decrease in spine density compared to DMSO-injected WT mice which was rescued by salubrinal treatment (salubrinal Tg2576 vs DMSO Tg2576 mice, $p < .05$; salubrinal Tg2576 mice vs DMSO WT mice, $p < .05$).

3.9. Salubrinal rescues novel object recognition performance and neuronal activity

Early synaptic deficits shown by Tg2576 mice correlate with impairments in hippocampal-dependent tasks. Accordingly, we probed whether rescuing the plasticity and morphology of hippocampal synapses also rescued novel object recognition performance in 3 month-old mice (Fig. 5). During the training phase (Fig. 5B), no difference was detected in the rate of exploration of the two identical objects in any group (DMSO WT: object sx vs object dx, $t_{(10)} = 0,10$, $p = 0,9$; DMSO Tg2576: object sx vs object dx, $t_{(8)} = 1,66$, $p = .13$; salubrinal WT: object sx vs object dx, $t_{(14)} = 0,84$; $p = 0,42$; salubrinal Tg2576: object sx vs object dx $t_{(10)} = 1,87$; $p = 0,09$). Differently, during the test phase (Fig. 5C) only DMSO Tg2576 mice failed to explore more the novel (NO) than the familiar (FO) object (DMSO Tg2576: NO vs FO, $t_{(8)} = 0,29$, $p = 0,77$; DMSO WT: NO vs FO $t_{(12)} = 3,86$; $p = .1$; salubrinal WT: NO vs FO $t_{(16)} = 2,18$; $p = .04$; salubrinal Tg2576: NO vs FO, $t_{(18)} = 3,65$; $p < .01$). Based on data showing that Tg2576 mice show defective activation of hippocampal neurons during formation or retrieval of hippocampal-dependent memory (Broadbent et al., 2004; Lelos and Good, 2014), and that healthy mice exposed to the NOR test show hippocampal neuronal activation (Tanimizu et al., 2017), we visualized by immunofluorescence the protein *c-fos* proto-oncogene in the CA1 region 1 h after NOR test (Fig. 5D). A two-way ANOVA carried out on the number of immunoreactivity spots detected in the CA1 region of the four experimental groups revealed a significant genotype × treatment interaction ($F_{(1,22)} = 8,04$; $p = .01$). Pair comparisons showed a lower number of *c-fos* immunoreactive spots in DMSO Tg2576 mice compared with DMSO WT mice ($p < .001$) that was rescued by salubrinal treatment (salubrinal Tg2576 vs DMSO WT mice, $P = 0,76$). No effect of treatment was detected on *c-fos* expression in the wild-type mice (salubrinal WT vs DMSO WT $p = 0,83$).

4. Discussion

The main finding of this study is that polysomal APP signals associated with decreased values of the p-eIF2α/eIF2α ratio were exclusively detected in pre-symptomatic 1-month old and early symptomatic 3-month old mutant mice. Differently, the absence of polysomal APP signals was associated with increased values of the p-eIF2α/eIF2α ratio in symptomatic 6- and 9-month old mice.

It is therefore apparent that the phosphorylation status of eIF2α varies according to the progression of AD pathogenesis with an early unbalance in favor of decreased phosphorylation, which enhances overall translation, followed by a late unbalance in favor of increased phosphorylation, which decreases overall translation. Interestingly, we found no evidence of alteration in other main players of translation initiation including the phosphorylated and non-phosphorylated states of the eukaryotic translation initiation factor 4E (p-eIF4E and eIF4E), and the non-phosphorylated state of the eukaryotic translation initiation factor 4G (eIF4G) which confirm the relevance of a single

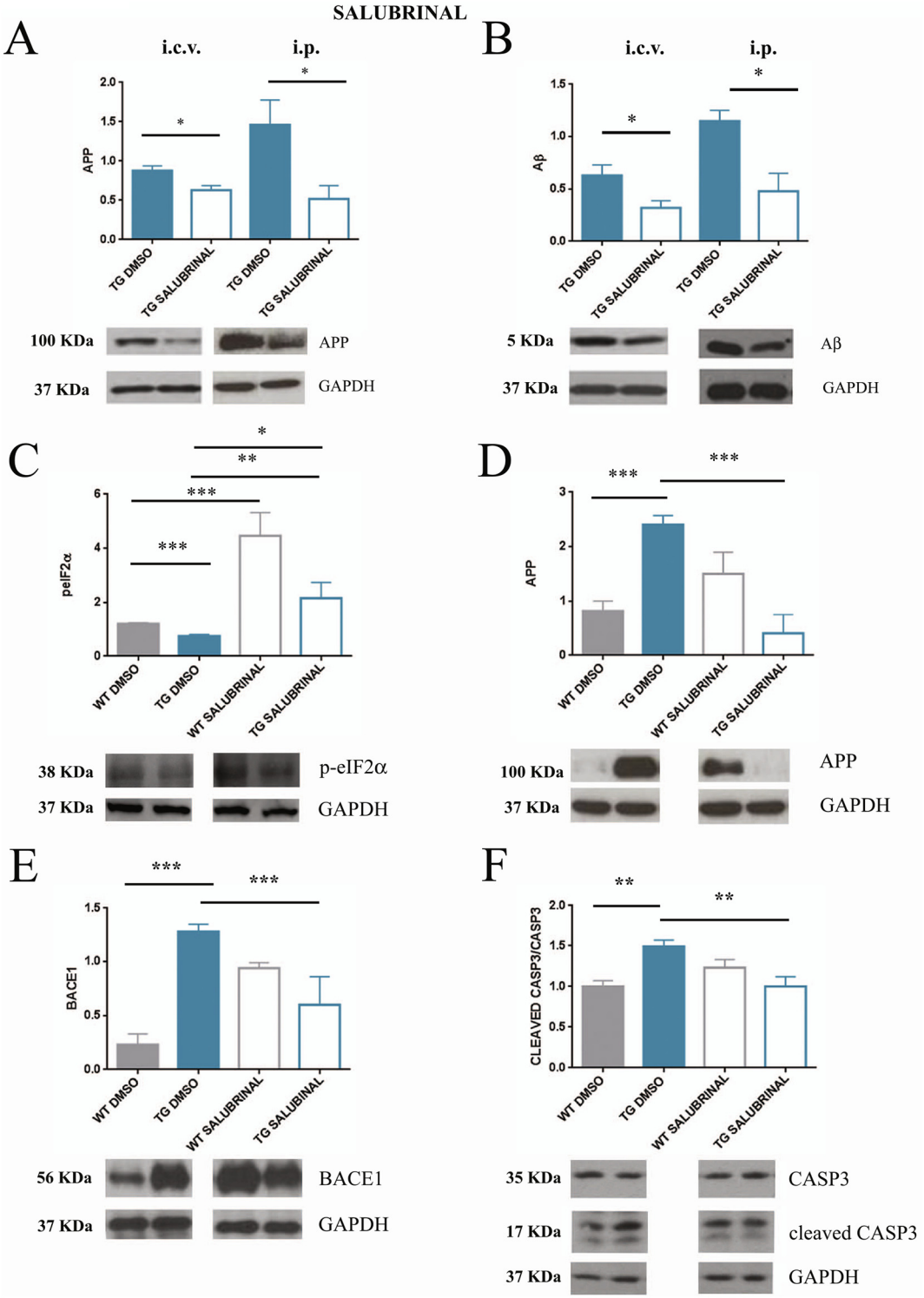

Fig. 3. Salubrinal rescues pathogenic AD markers in the hippocampus of 3-month old Tg2576 mice. Histograms showing that i.c.v. (1 μl of a 75 μM solution diluted in DMSO) or i.p. (1 mg/kg diluted in DMSO repeated for 7 consecutive days) injections of salubrinal were effective in decreasing **(A)** APP and **(B)** Aβ levels in the hippocampus of Tg2576 mice. Histograms showing that i.p. injections of salubrinal were effective in restoring proper levels of **(C)** eIF2α **(D)** APP, **(E)** beta-secretase 1 (BACE-1) in hippocampal extracts, and **(F)** of caspase-3 in hippocampal synaptosomes of 3-month old Tg2576 mice. Bars represent mean ± SEM. (Tg2576 DMSO: solid blue bars; Tg2576 salubrinal: empty blue bars; wild-type DMSO: solid grey bars; wild-type salubrinal: empty grey bars) $*p < .05$; $** p < 0.01$; $***p < 0{,}001$). (For interpretation of the references to colour in this figure legend, the reader is referred to the web version of this article.)

phosphorylation site in eIF2α as a key regulator of cognitive processes (Costa-Mattioli et al., 2007).

Phosphorylation of the α-subunit of eukaryotic initiation factor 2 (eIF2α) acts as a negative regulator of general translation (Donnelly et al., 2013; Ohno, 2014). In AD, there is evidence that accumulation of Aβ increases eIF2α phosphorylation which then blocks mRNA translation and de novo protein synthesis. This has been shown in cultured cells expressing swe-hAPP, in mature cultured hippocampal neurons exposed to Aβ oligomers (Lourenco et al., 2013) and in brain tissues from sporadic AD patients (Kim et al., 2007; Chang et al., 2002; Segev

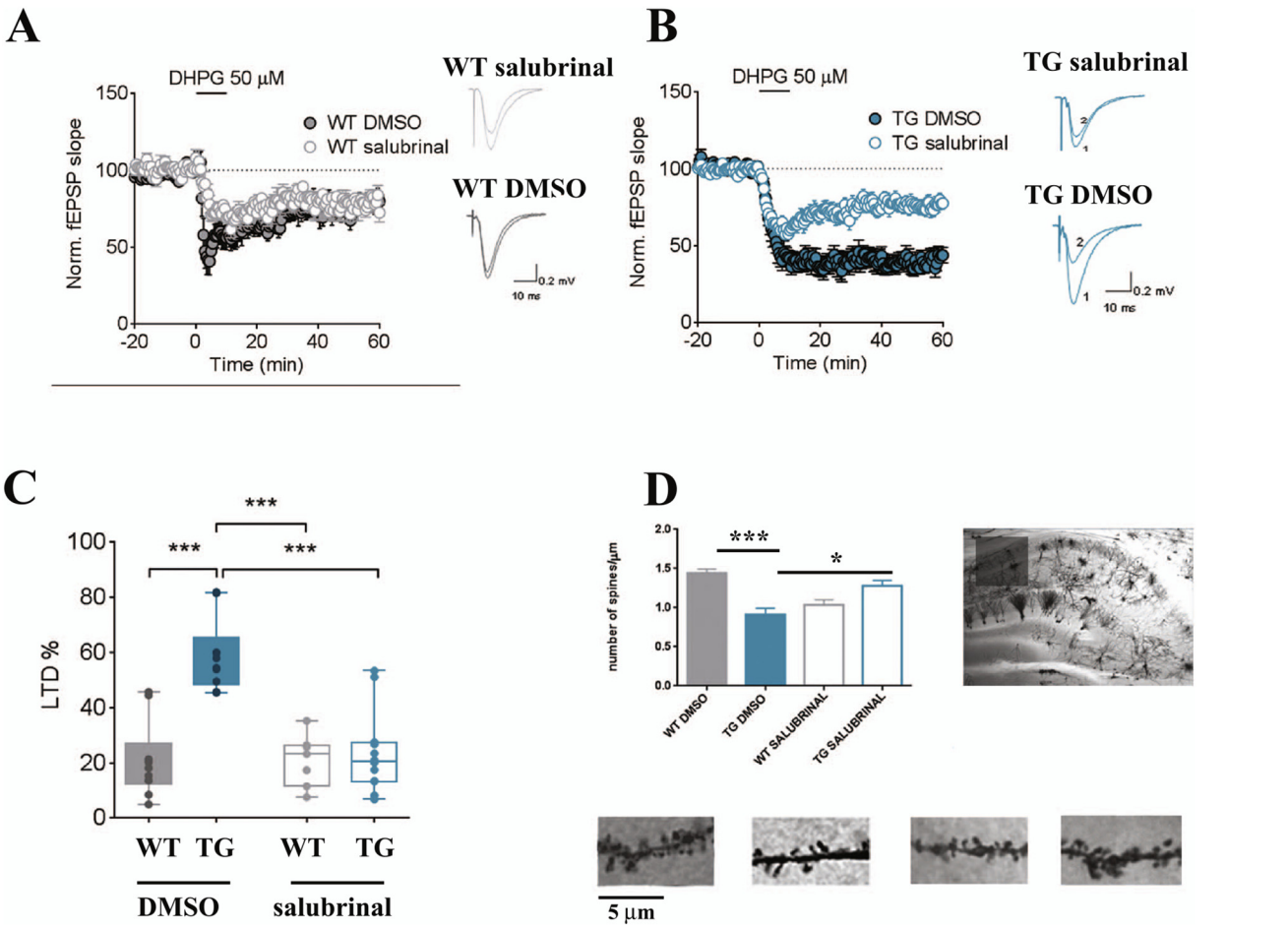

Fig. 4. Salubrinal rescues hippocampal CA1 dendritic spine loss and increased LTD at CA3-CA1 hippocampal synapses. Superimposed fEPSPs traces recorded immediately before DHPG (50 μM, 10 min) and at 55–60 min of DHPG washout in 3-month-old saline and salubrinal-treated WT **(A)** and Tg2576 (TG) mice **(B).** Running plots show normalized fEPSP mean slope (± SEM. displayed every 1.5 min) recorded from the dendritic region of CA1 neurons in hippocampal slices from WT and TG mice exposed to 50 μM DHPG for 10 min. **(C)** The box-and-whisker plot indicates the degree of DHPG-LTD, measured as fEPSP slope decrease from baseline, 55–60 min from DHPG washout (WT: $n = 10$ slices from 4 saline, 7 slices from 4 salubrinal-treated mice; Tg2576: n = 10 slices from 4 saline, 12 slices from 4 salubrinal-treated mice). *** $p < 0{,}001$ **(D)** Left: Histograms showing dendritic spines (number of spines/dendrite segment length) counted on 5 segments per neuron in 10 pyramidal neurons laying in the CA1 subfield of the hippocampus in wild-type mice (grey bars) and Tg2576 mice (blue bars) injected with DMSO (solid bars) or salubrinal (empty bars). Bars represent mean ± SEM. Right: representative images of Golgi-stained sections of the dorsal hippocampus (scale bar: 10 μm) and of apical dendrite segments of CA1 hippocampal pyramidal neurons (scale bar: 10 μm) in 3-month-old wild-type and Tg2576 mice injected with DMSO or salubrinal. ***$p < .001$. (For interpretation of the references to colour in this figure legend, the reader is referred to the web version of this article.)

et al., 2013) and from symptomatic AD mice expressing the hAPP mutation alone (Kim et al., 2007) or in association with other mutant proteins (Devi and Ohno, 2010; Devi and Ohno, 2010a; Devi and Ohno, 2013; Page et al., 2006). Accordingly, the enhancement of p-eIF2α levels in symptomatic AD patients and mouse models has been essentially considered as the mechanism which mediates cognitive deterioration via reduced translation and expression of synaptic plasticity proteins. More recently, however, elevated levels of eIF2α phosphorylation have been shown to elicit the unfolded protein response in the hippocampus and the temporal cortex of AD patients (Hoozemans et al., 2005) which suggests that the downregulation of translation observed during the symptomatic phase can also be viewed as a prominent neuroprotective mechanisms aimed at restoring normal cell function. Thus, a possible explanation for the fluctuation of p-eIF2α levels in the mutant mice could be that the prodromal and early symptomatic decrease of p-eIF2α which favors APP accumulation, is then contrasted by a compensatory decrease which restricts APP accumulation.

Having identified an early symptomatic age point (3 months) wherein eIF2α is decreased, APP mRNA and protein are increased, and Aβ oligomers become detectable, we then examined whether inhibiting eIF2α dephosphorylation, i.e., decreasing overall translation, could prevent the elevation of APP and Aβ levels. We tested this hypothesis by injecting the selective inhibitor of eIF2α dephosphorylation salubrinal both i.c.v. and i.p. in 3-month old mutants and found that, whatever the injection route, salubrinal significantly lowered hippocampal APP and C-terminal Aβ levels. Our findings are in line with in vitro data which show that short-term treatment with salubrinal attenuates Aβ-induced neuronal death in primary cortical neuronal cells (Huang et al., 2012), and with several in vitro and in vivo data which indicate that compounds like MMP13, which regulates BACE-1 translation, or posiphen, which decreases the production of toxic Aβ by lowering APP translation, are effective in rescuing cognitive deficits in hAPP mutant AD mice (Lahiri et al., 2007) and sporadic AD patients (Teich et al., 2018).

We therefore verified whether salubrinal chronically administered in 3-month old mutants via the less invasive intraperitoneal injection route could restore physiological levels of those and other major pathogenic AD markers. We first observed that hippocampal levels of APP, Aβ, BACE-1 measured in salubrinal-injected Tg2576 mice no longer differed from those measured in vehicle-injected WT mice. We also noticed a rescue of previously reported synaptic alterations (D'Amelio

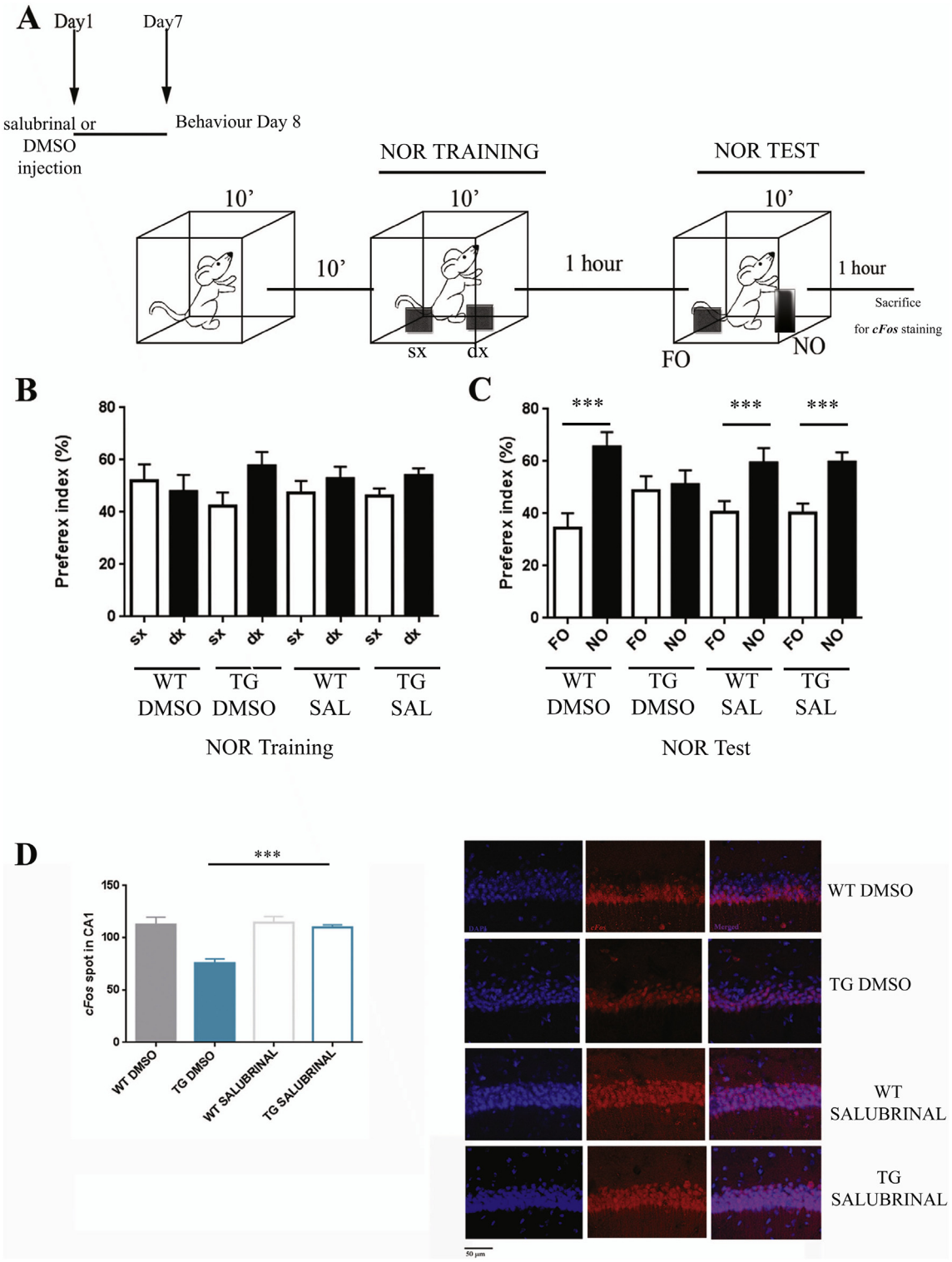

Fig. 5. Salubrinal rescues novel object recognition deficit in Tg2576 mice (A) Cartoon depicting the behavioral protocol. Tg2576 mice were injected daily with salubrinal (i.p., 1 mg/kg) or with the same volume of DMSO during 7 consecutive days and their performance in the novel object recognition (NOR) task was compared with the performance of wild-type (WT) mice injected with DMSO. Mice were first exposed to two identical objects (training) and, 1 h after, one of familiar object was substituted with a novel object (testing). The time spent exploring each object was recorded during each phase and the preference index for each object was calculated (time exploring one object divided by the time exploring the two objects*100). (**B**) Histograms showing the preference index for object sx (left, white bars) and dx (right, black bars) during training. No effect of genotype or treatment was found (**C**) Histograms showing the preference index for object FO (familiar object) and object NO (novel object). Tg2576 mice injected with DMSO showed the same preference index for objects FO and NO. Differently, Tg2576 mice injected with salubrinal, and wild-type mice injected with DMSO explored significantly more object NO than object FO. (**D**) Histograms (left) and representative c-fos immunohistochemistry staining (right) showing the number of c-fos positive spots in the CA1 region of the hippocampus (10 areas of 25 × 25 μm in size per mouse) of DMSO-injected wild-type (grey solid bars) and Tg2576 (blue solid bars), and in salubrinal injected wild-type (grey empty bars) and Tg2576 (blue empty bars) mice. Bars represent mean ± SEM. *$p < .05$. (For interpretation of the references to colour in this figure legend, the reader is referred to the web version of this article.)

et al., 2011) including the enhancement of caspase-3 in hippocampal synaptosomes, the prevalence of LTD at hippocampal synapses, and the decrease in dendritic spines in CA1 hippocampal pyramidal neurons. We then found that the treatment could prevent performance impairments in the NOR task, and restored NOR-induced hippocampal *c-fos* activation. These effects were specific to Tg2576 mice as, in line with the Mouton-Liger et al. (2012) who reported an augmentation of BACE-1 levels and amyloidogenesis in salubrinal-injected healthy mice, we found an increase in APP, Aβ and peIF2α levels in WT mice following both i.c.v. and i.p, administration of the compound. Also, partially consistent with the report that salubrinal abolishes late-LTP and disrupts long term contextual memory in healthy mice (Costa-Mattioli et al., 2007, Lourenco et al., 2013), we observed a marginal significant reduction in dendritic spines but no disruption of NOR performance or NOR-induced hippocampal *c-fos* activation in salubrinal–injected WT mice. Differences in the injection protocols (single post-training hippocampal bilateral infusion vs chronic pre-training injections) and the learning tasks (associative vs non associative) that were used likely account for the discrepancies between the Costa-Mattioli et al. (2007) and the present data. Also, genotypic differences in hippocampal function might explain why the same route and regimen of salubrinal injections disrupts memory performance in outbred Swiss mice (Lourenco et al., 2013) but did not in our wild-type C7BL/6 (B6) x SJL inbred mice which, due to their half B6 background, should outperform in hippocampus-dependent tasks (Paylor et al., 1994; Crawley et al., 1997) and form more resistant memories. Nevertheless, the three studies converge in showing that salubrinal injected in healthy mice triggers a pattern of AD-related pathogenic neural factors similar to the one exhibited by fully symptomatic APP mutant mice.

Altogether, our findings show an early upregulation of translational efficiency in Tg2576 mice which, by favoring hAPP overexpression, contributes to precipitate the transition between the early symptomatic and the symptomatic phase. Remarkably, repression of overall translation by salubrinal treatment at the onset of AD-like symptoms prevents the release of toxic products (Aβ) or apoptotic factors (caspase-3), but also reinstates APP physiological processing via concurrent regularization of APP and BACE-1 levels. It is therefore apparent that the peIF2α–mediated regulation of APP processing by salubrinal is beneficial during the time-window where Tg2576 mice exhibit a transient rise in overall translation.

Of note, altered mechanisms of protein synthesis have been reported in the hippocampus of AD patients examined at several stages (Hernández-Ortega et al., 2016). A progressive augmentation in eIF2α levels was found between stages III–IV and V–VI. Remarkably, alterations in the elongation factor eEF2 were even detected at that stage I-II thereby showing for the first time the presence of protein synthesis alterations at a very early stage of the disease. Alteration of genes involved in protein synthesis were further identified in the frontal cortex of both AD patients at advanced stages, and in fully symptomatic APP/PS1 mice (Garcia-Esparcia et al., 2017). Although no strict overlapping was found between the proteins which were altered in patients and mice, reduced protein levels of elongation factor eEF2 repressing translational efficiency was identified as a common mechanism. These findings, together with our observations, strongly suggest that intercepting and correcting time-widow/direction-specific alterations in translational efficiency might represent a powerful tool to prevent or contrast AD.

The following are the supplementary data related to this article.

Ethical approval

All protocols involving animals were performed in accordance with the guidelines established by the European Communities Council (Directive 2010/63/EU of 22 September 2010). Experiments involving animals were performed in accordance with the relevant approved guidelines and regulations accepted by the Italian Ministry of Health and approved by the Ethical Committee on Animal Experiments of Rome, Italy.

Authors contribution

A.B. conceived and designed the research plan, supervised the molecular, anatomical, and behavioral experiments, and wrote the manuscript. F.V., L.E., M.D.L. carried out polysome profiling, western blot, behavioral, anatomical, and c-fos experiments. A.R. performed eIF4G and eIF4E analyses. A.C. run the electrophysiological experiments under the N.B.M supervision. V.C. and GA performed p-eIF2α measurements in 3-month old mice. A.N. performed caspase-3 analysis in hippocampal synaptosomes under the M.D.A. supervision. M.D.A. critically read the manuscript. M.A.T. supervised the research plan and wrote the manuscript.

Supplementary data to this article can be found online at https://doi.org/10.1016/j.nbd.2020.104787

Declaration of Competing Interest

The authors have no conflict of interest to disclose.

Acknowledgements

This work was supported by a grant (AGESPAN) from CNR-National Research Council of Italy to M A-T. A.B. was supported by Fondazione Umberto Veronesi. A.B also got FRAXA Research Foundation award. MDA was supported by the Italian Ministry of Health (Progetto Ricerca Finalizzata project code RF-2018-12365527) and by a grant from the Alzheimer's Association, United States (Project Code AARG-18-566270). A.N. was supported by a post-doctoral fellowship by the Collegio Ghislieri. We thank Marcello Ceci for technical support with polysome gradient machinery and Stefano Biffo for scientific support and constructive reading of the manuscript.

References

Antunes, M., Biala, G., 2012. The novel object recognition memory: neurobiology, test procedure, and its modifications. Cogn. Process. 13 (2), 93–110. https://doi.org/10.1007/s10339-011-0430-z.

Beason-Held, L.L., Goh, J.O., An, Y., Kraut, M.A., O'Brien, R.J., Ferrucci, L., et al., 2013 Nov 13. Changes in brain function occur years before the onset of cognitive impairment. J. Neurosci. 33 (46), 18008–18014. https://doi.org/10.1523/JNEUROSCI.1402-13.2013.

Borreca, A., Gironi, K., Amadoro, G., Ammassari-Teule, M., 2016 Jul. Opposite dysregulation of fragile-X mental retardation protein and heteronuclear ribonucleoprotein C protein associates with enhanced APP translation in Alzheimer disease. Mol. Neurobiol. 53 (5), 3227–3234. https://doi.org/10.1007/s12035-015-9229-8.

Borreca, A., Latina, V., Corsetti, V., Middei, S., Piccinin, S., Della Valle, F., et al., 2018 Oct. AD-related N-terminal truncated tau is sufficient to recapitulate in vivo the early perturbations of human neuropathology: implications for immunotherapy. Mol. Neurobiol. 55 (10), 8124–8153. https://doi.org/10.1007/s12035-018-0974-3.

Broadbent, N.J., Squire, L.R., Clark, R.E., 2004. Spatial memory, recognition memory, and the hippocampus. Proc. Natl. Acad. Sci. U. S. A. 101 (40), 14515–14520. https://doi.org/10.1073/pnas.0406344101.

Caccamo, A., Branca, C., Talboom, J.S., Shaw, D.M., Turner, D., Ma, L., et al., 2015. Reducing ribosomal protein S6 kinase 1 expression improves spatial memory and synaptic plasticity in a mouse model of Alzheimer's disease. J. Neurosci. 35 (41), 14042–14056. https://doi.org/10.1523/JNEUROSCI.2781-15.2015.

Chang, R.C., Wong, A.K., Ng, H.K., Hugon, J., 2002 Dec 20. Phosphorylation of eukaryotic initiation factor-2a (eIF2α) is associated with neuronal degeneration in Alzheimer's disease. Neuroreport. 13 (18), 2429–2432. https://doi.org/10.1097/01.wnr.0000048020.74602.bb.

Costa-Mattioli, M., Gobert, D., Stern, E., Gamache, K., Colina, R., Cuello, C., et al., 2007 Apr 6. eIF2alpha phosphorylation bidirectionally regulates the switch from short- to long-term synaptic plasticity and memory. Cell. 129 (1), 195–206. https://doi.org/10.1016/j.cell.2007.01.050.

Coxon, F.P., Benford, H.L., Russell, R.G., Rogers, M.J., 1998 Oct. Protein synthesis is required for caspase activation and induction of apoptosis by bisphosphonate drugs. Mol. Pharmacol. 54 (4), 631–638.

Crawley, J.N., Belknap, J.K., Collins, A., Crabbe, J.C., Frankel, W., et al., 1997. Behavioral phenotypes of inbred mouse strains: implications and recommendations for molecular studies. Psychopharmacol. 132 (2), 107–124. https://doi.org/10.1007/s002130050327.

D'Amelio, M., Cavallucci, V., Middei, S., Marchetti, C., Pacioni, S., Ferri, A., et al., 2011. Caspase-3 triggers early synaptic dysfunction in a mouse model of Alzheimer's disease. Nat. Neurosci. 14 (1), 69–76. https://doi.org/10.1038/nn.2709.

Devi, L., Ohno, M., 2010. Phospho-eIF2α level is important for determining abilities of BACE1 reduction to rescue cholinergic neurodegeneration and memory defects in 5XFAD mice. PLoS One 5 (9), e12974. https://doi.org/10.1371/journal.pone.0012974.

Devi, L., Ohno, M., 2010a. Genetic reductions of beta-site amyloid precursor protein-cleaving enzyme 1 and amyloid-beta ameliorate impairment of conditioned taste aversion memory in 5XFAD Alzheimer's disease model mice. Eur. J. Neurosci. 31 (1), 110–118. https://doi.org/10.1111/j.1460-9568.2009.07031.x.

Devi, L., Ohno, M., 2013. Deletion of the eIF2a kinase GCN2 fails to rescue the memory decline associated with Alzheimer's disease. PLoS One 8 (10), e77335. https://doi.org/10.1371/journal.pone.0077335.

Donnelly, N., Gorman, A.M., Gupta, S., Samali, A., 2013. The eIF2α kinases: their structures and functions. Cell. Mol. Life Sci. 70 (19), 3493–3511. https://doi.org/10.1007/s00018-012-1252-6.

Garcia-Esparcia, P., Sideris-Lampretsas, G., Hernandez-Ortega, K., Grau-Rivera, O., Sklaviadis, T., Gelpi, E., et al., 2017 Jun 15. Altered mechanisms of protein synthesis in frontal cortex in Alzheimer disease and a mouse model. Am. J. Neurodegener. Dis. 6 (2), 15–25.

Georgievska, B., Gustavsson, S., Lundkvist, J., Neelissen, J., Eketjäll, S., Ramberg, V., et al., 2015. Revisiting the peripheral sink hypothesis: inhibiting BACE1 activity in the periphery does not alter β-amyloid levels in the CNS. J. Neurochem. 132 (4), 477–486. https://doi.org/10.1111/jnc.12937.

Gibb, R., Kolb, B., 1998. A method for vibratome sectioning of Golgi-Cox stained whole rat brain. J. Neurosci. Methods 79 (1), 1–4. https://doi.org/10.1016/s0165-0270(97)00163-5.

Gong, N., Wu, J.H., Liang, Z.S., Jiang, W.H., Wang, X.W., Scheff, S.W., et al., 2015. Role of salubrinal in protecting cardiomyocytes from doxorubicin-induced apoptosis. Genet. Mol. Res. 14 (4), 12377–12385. https://doi.org/10.4238/2015.

Grüner, S., Peter, D., Weber, R., Wohlbold, L., Chung, M.Y., Weichenrieder, O., et al., 2016 Nov 3. The structures of eIF4E-eIF4G complexes reveal an extended interface to regulate translation initiation. Mol. Cell 64 (3), 467–479. https://doi.org/10.1016/j.molcel.2016.09.020.

Head, E., Helman, A.M., Powell, D., Schmitt, F.A., 2018 Jan. Down syndrome, beta-amyloid and neuroimaging. Free Radic. Biol. Med. 114, 102–109. https://doi.org/10.1016/j.freeradbiomed.2017.09.013.

Hernández-Ortega, K., Garcia-Esparcia, P., Gil, L., Lucas, J.J., Ferrer, I., 2016 Sep. Altered machinery of protein synthesis in Alzheimer's: from the nucleolus to the ribosome. Brain Pathol. 26 (5), 593–605. https://doi.org/10.1111/bpa.12335.

Hoozemans, J.J., Veerhuis, R., Van Haastert, E.S., Rozemuller, J.M., Baas, F., Eikelenboom, P., et al., 2005 Aug. The unfolded protein response is activated in Alzheimer's disease. Acta Neuropathol. 110 (2), 165–172. https://doi.org/10.1007/s00401-005-1038-0.

Howlett, D.R., Richardson, J.C., 2009. The pathology of APP transgenic mice: a model of Alzheimer's disease or simply overexpression of APP? Histol. Histopathol. 24 (1), 83–100. https://doi.org/10.14670/HH-24.83.

Huang, X., Chen, Y., Zhang, H., Ma, Q., Zhang, Y.W., Xu, H., 2012 May. Salubrinal attenuates β-amyloid-induced neuronal death and microglial activation by inhibition of the NF-κB pathway. Neurobiol. Aging 33 (5). https://doi.org/10.1016/j.neurobiolaging.2011.10.007. (1007.e9-17).

Johnston, J.A., Cowburn, R.F., Norgren, S., Wiehager, B., Venizelos, N., Winblad, B., et al., 1994. Increased β-amyloid release and levels of amyloid precursor protein (APP) in fibroblast cell lines from family members with the Swedish Alzheimer's disease APP670/671 mutation. FEBS Lett. 354 (3), 274–278. https://doi.org/10.1016/0014-5793(94)01137-0.

Kim, H.S., Choi, Y., Shin, K.Y., Joo, Y., Lee, Y.K., Jung, S.Y., et al., 2007 May 15. Swedish amyloid precursor protein mutation increases phosphorylation of eIF2a in vitro and in vivo. J. Neurosci. Res. 85 (7), 1528–1537. https://doi.org/10.1002/jnr.21267.Y, 2007.

Lahiri, D.K., Chen, D., Maloney, B., Holloway, H.W., Yu, Q.S., Utsuki, T., et al., 2007 Jan. The experimental Alzheimer's disease drug posiphen [(+)-phenserine] lowers amyloid-beta peptide levels in cell culture and mice. Pharmacol. Exp. Ther. 320 (1), 386–396. https://doi.org/10.1124/jpet.106.112102.

Lanté, F., Raymodg, E.F., Salgueiro-Pereira, A.R., Mouska, X., Kootar, S., Barik, J., et al., 2015. Subchronic glucocorticoid receptor inhibition rescues early episodic memory and synaptic plasticity deficits in a mouse model of Alzheimer's disease. Neuropsychopharmacology 40 (7), 1772–1781. https://doi.org/10.1038/npp.2015.25.

Lee, E.K., Kim, H.H., Kuwano, Y., Abdelmohsen, K., Srikantan, S., Subaran, S.S., et al., 2010. hnRNP C promotes APP translation by competing with FMRP for APP mRNA recruitment to P bodies. Nat. Struct. Mol. Biol. 17 (6), 732–739. https://doi.org/10.1038/nsmb.1815.

Lelos, M.J., Good, M.A., 2014 May. β-Amyloid pathology alters neural network activation during retrieval of contextual fear memories in a mouse model of Alzheimer's disease. Eur. J. Neurosci. 39 (10), 1690–1703. https://doi.org/10.1111/ejn.12527.

Long, J.M., Ray, B., Lahiri, D.K., 2012. MicroRNA-153 physiologically inhibits expression of amyloid-β precursor protein in cultured human fetal brain cells and is dysregulated in a subset of Alzheimer disease patients. J. Biol. Chem. 287 (37), 31298–31310. https://doi.org/10.1074/jbc.M112.366336.

Lourenco, M.V., Clarke, J.R., Frozza, R.L., Bomfim, T.R., Forny-Germano, L., Batista, A.F., et al., 2013 Dec 3. TNF-α mediates PKR-dependent memory impairment and brain IRS-1 inhibition induced by Alzheimer's β-amyloid oligomers in mice and monkeys. Cell Metab. 18 (6), 831–843. https://doi.org/10.1016/j.cmet.2013.11.002.

Maloney, B., Lahiri, D.K., 2016 Jun. Epigenetics of dementia: understanding the disease as a transformation rather than a state. Lancet Neurol. 15 (7), 760–774. https://doi.org/10.1016/S1474-4422(16)00065-X.

Mouton-Liger, F., Paquet, C., Dumurgier, J., Bouras, C., Pradier, L., Gray, F., et al., 2012. Oxidative stress increases BACE1 protein levels through activation of the PKR- eIF2a pathway. Biochim. Biophys. Acta 1822 (6), 885–896. https://doi.org/10.1016/j.bbadis.2012.01.009.

Neumann, U., Rueeger, H., Machauer, R., Veenstra, S.J., Lueoend, R.M., Tintelnot-Blomley, M., et al., 2015. A novel BACE inhibitor NB-360 shows a superior pharmacological profile and robust reduction of amyloid-β and neuroinflammation in APP transgenic mice. Mol. Neurodegener. 10, 44. https://doi.org/10.1186/s13024-015-0033-8.

Ohno, M., 2014. Roles of eIF2α kinases in the pathogenesis of Alzheimer's disease. Front. Mol. Neurosci. 7, 22. https://doi.org/10.3389/fnmol.2014.00022.

Page, G., Rioux Bilan, A., Ingrand, S., Lafay-Chebassier, C., Pain, S., Perault Pochat, M.C., et al., 2006. Activated double-stranded RNA-dependent protein kinase and neuronal death in models of Alzheimer's disease. Neuroscience. 139 (4), 134354. https://doi.org/10.1016/j.neuroscience.2006.01.047.

Paylor, R., Tracy, R., Wehner, J., Rudy, J.W., 1994. DBA/2 and C57BL/6 mice differ in contextual fear conditioning but not auditory fear conditioning. Behav Neurosci. 108 (4), 810–817.

Pignataro, A., Meli, G., Pagano, R., Fontebasso, V., Battistella, R., Conforto, G., et al., 2019 Aug 1. Activity-induced amyloid-β oligomers drive compensatory synaptic rearrangements in brain circuits controlling memory of presymptomatic Alzheimer's disease mice. Biol. Psychiatry 86 (3), 185–195. https://doi.org/10.1016/j.biopsych.2018.10.018.

Ray, B., Long, J.M., Sokol, D.K., Lahiri, D.K., 2011. Increased secreted amyloid precursor protein-α (sAPPα) in severe autism: proposal of a specific, anabolic pathway and putative biomarker. PLoS One 6 (6), e20405. https://doi.org/10.1371/journal.pone.0020405.

Richter, J.D., Sonenberg, N., 2005 Feb 3. Regulation of cap-dependent translation by eIF4E inhibitory proteins. Nature. 433 (7025), 477–480. https://doi.org/10.1038/nature03205.

Scheff, S.W., Price, D.A., Schmitt, F.A., DeKosky, S.T., Mufson, E.J., 2007. Synaptic alterations in CA1 in mild Alzheimer disease and mild cognitive impairment. Neurology. 68 (18), 1501–1508. https://doi.org/10.1212/01.wnl.0000260698.46517.8f.

Segev, Y., Michaelson, D.M., Rosenblum, K., 2013. ApoE ε4 is associated with eIF2a phosphorylation and impaired learning in young mice. Neurobiol. Aging 34 (3), 863–872. https://doi.org/10.1016/j.neurobiolaging.2012.06.020.

Sokka, A.L., Putkonen, N., Mudo, G., Pryazhnikov, E., Reijonen, S., Khiroug, L., et al., 2007 Jan 24. Endoplasmic reticulum stress inhibition protects against excitotoxic neuronal injury in the rat brain. J. Neurosci. 27 (4), 901–908. https://doi.org/10.1523/JNEUROSCI.4289-06.2007.

Sokol, D.K., Chen, D., Farlow, M.R., Dunn, D.W., Maloney, B., Zimmer, J.A., et al., 2006 Jun. High levels of Alzheimer beta-amyloid precursor protein (APP) in children with severely autistic behavior and aggression. J. Child Neurol. 21 (6), 444–449. https://doi.org/10.1177/08830738060210062201.

Tanimizu, T., Kono, K., Kida, S., 2017. Brain networks activated to form object recognition memory. Brain Res. Bull. https://doi.org/10.1016/j.brainresbull.2017.05.017. pii: S0361-9230(17)30219-8.

Tcw, J., Goate, A.M., 2017 Jun 1. Genetics of β-amyloid precursor protein in Alzheimer's disease. Cold Spring Harb. Perspect. Med. 7 (6). https://doi.org/10.1101/cshperspect.a024539. pii: a024539.

Teich, A.F., Sharma, E., Barnwell, E., Zhang, H., Staniszewski, A., Utsuki, T., et al., 2018 Jan 18. Translational inhibition of APP by posiphen: efficacy, pharmacodynamics, and pharmacokinetics in the APP/PS1 mouse. Alzheimers Dement (N Y) 4, 37–45. https://doi.org/10.1016/j.trci.2017.12.00.

Vignini, A., Morganti, S., Salvolini, E., Sartini, D., Luzzi, S., Fiorini, R., et al., 2013. Amyloid precursor protein expression is enhanced in human platelets from subjects with Alzheimer's disease and frontotemporal lobar degeneration: a real-time PCR study. Exp. Gerontol. 48 (12), 1505–1508.

Westmark, C.J., 2019. Fragile X and APP: a decade in review, a vision for the future. Mol. Neurobiol. 56, 3904–3921. https://doi.org/10.1007/s12035-018-1344-x.

Westmark, C.J., Sokol, D.K., Maloney, B., Lahiri, D.K., 2016 Oct. Novel roles of amyloid-beta precursor protein metabolites in fragile X syndrome and autism. Mol. Psychiatry 21 (10), 1333–1341. https://doi.org/10.1038/mp.2016.134.

Zhu, B.L., Long, Y., Luo, W., Yan, Z., Lai, Y.J., Zhao, L.G., et al., 1 January 2019. MMP13 inhibition rescues cognitive decline in Alzheimer transgenic mice via BACE1 regulation. Brain 142 (1), 176–192. https://doi.org/10.1093/brain/awy305.